ORIGINAL RESEARCH

Neem Oil or Almond Oil Nanoemulsions for Vitamin E Delivery: From Structural Evaluation to in vivo Assessment of Antioxidant and Anti-Inflammatory Activity

Federica Rinaldi[1,]*, Patrizia Nadia Hanieh[1,]*, Linda Maurizi[2], Catia Longhi[2], Daniela Uccelletti[3], Emily Schifano[3], Elena Del Favero [4], Laura Cantù[4,†], Caterina Ricci[4], Maria Grazia Ammendolia[5], Donatella Paolino[6], Francesca Froiio[6], Carlotta Marianecci[1], Maria Carafa [1]

[1]Dipartimento di Chimica e Tecnologie del Farmaco, Sapienza Università di Roma, Rome, Italy; [2]Dipartimento di Sanità pubblica e Malattie infettive, Sapienza Università di Roma, Rome, Italy; [3]Dipartimento di Biologia e Biotecnologie Charles Darwin, Sapienza Università di Roma, Rome, Italy; [4]Dipartimento di Biotecnologie Mediche e Medicina Traslazionale, Università di Milano, Milan, Italy; [5]Centro Nazionale Tecnologie Innovative in Sanità Pubblica, Istituto Superiore di Sanità, Rome, Italy; [6]Dipartimento di Medicina Sperimentale e Clinica, Università Magna Graecia di Catanzaro, Campus Universitario "S. Venuta", Catanzaro, Italy

*These authors contributed equally to this work
†Professor Laura Cantù passed away on August 05, 2022

Correspondence: Maria Carafa; Carlotta Marianecci, Dipartimento di Chimica e Tecnologie del Farmaco, Sapienza Università di Roma, Piazzale Aldo Moro 5, Roma, 00185, Italy, Tel +390649913603; +390649913970, Fax +39064913133, Email maria.carafa@uniroma1.it; carlotta.marianecci@uniroma1.it

Purpose: Vitamin E (VitE) may be classified in "the first line of defense" against the formation of reactive oxygen species. Its inclusion in nanoemulsions (NEs) is a promising alternative to increase its bioavailability. The aim of this study was to compare O/W NEs including VitE based on Almond or Neem oil, showing themselves antioxidant properties. The potential synergy of the antioxidant activities of oils and vitamin E, co-formulated in NEs, was explored.

Patients and Methods: NEs have been prepared by sonication and deeply characterized evaluating size, ζ-potential, morphology (TEM and SAXS analyses), oil nanodroplet feature, and stability. Antioxidant activity has been evaluated in vitro, in non-tumorigenic HaCaT keratinocytes, and in vivo through fluorescence analysis of *C. elegans* transgenic strain. Moreover, on healthy human volunteers, skin tolerability and anti-inflammatory activity were evaluated by measuring the reduction of the skin erythema induced by the application of a skin chemical irritant (methyl-nicotinate).

Results: Results confirm that Vitamin E can be formulated in highly stable NEs showing good antioxidant activity on keratinocyte and on *C. elegans*. Interestingly, only Neem oil NEs showed some anti-inflammatory activity on healthy volunteers.

Conclusion: From the obtained results, Neem over Almond oil is a more appropriate candidate for further studies on this application.

Keywords: O/W nanodispersion, α-tocopherol, anti-inflammatory activity, HaCaT, *C. elegans*, healthy volunteers

Introduction

Toxicity connected to reactive oxygen species (ROS) or free radicals arises under unbalanced conditions of biological systems, either because the protective mechanisms are impaired or an excessive production of free radicals overtakes the defense. Then, an excess of free radicals or their location at abnormal sites, following the unbalance between formation and removal, results in oxidative stress. Indeed, ROS and free radicals can attack molecules in their biological environment. To sum up, oxidative stress can be defined as a "state where oxidation exceeds the antioxidant systems because the balance between them has been lost".[1]

Oxidative stress may afflict all types of biological molecules and may be involved in processes such as carbohydrate and membrane damage, protein oxidation and fragmentation, lipid peroxidation, as well as mutagenesis and

Graphical Abstract
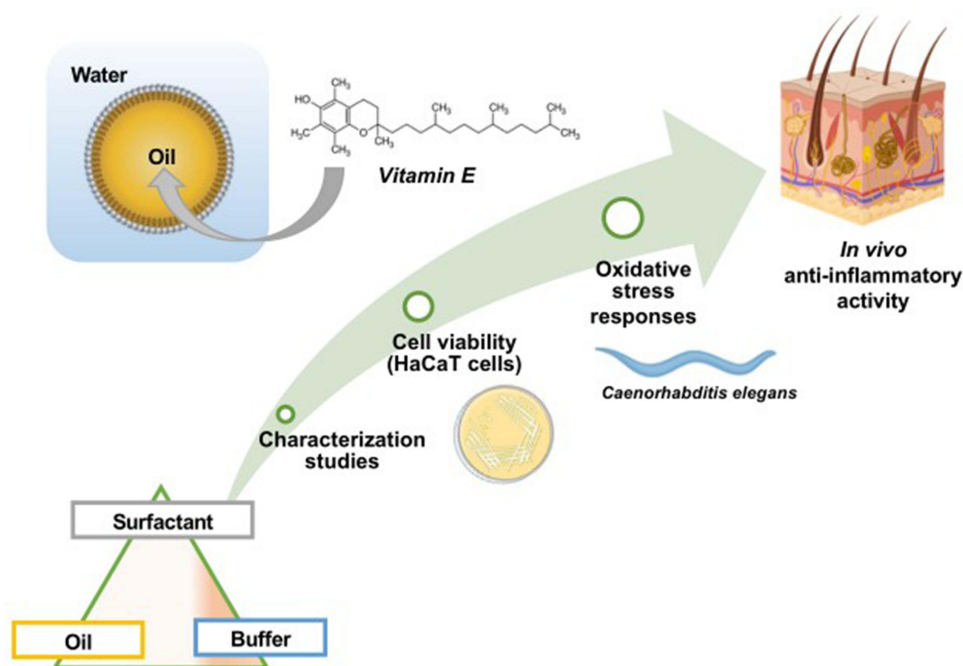
carcinogenesis. On the other hand, oxidative stress has a functional role: the presence of ROS at sites of inflammation can help modulate an excessive inflammatory response and kill pathogens, under certain circumstances.[2] This is a paradox in the free radical/antioxidant field that makes it a complex research field.[3–5]

Indeed, almost all aspects of aerobic life are concerned with free radicals and antioxidants.[6,7]

The absolute "best" antioxidant does not exist, with the best performance depending on the nature of the oxidative challenge.

Among non-enzymatic antioxidants, the Vitamins E and C as well as beta carotene may scavenge oxygen radicals. They can be classified in "the first line of defense" against ROS, that is, protection against their formation. In particular, α-tocopherol (VitE, Figure 1S) can be regarded as chain-breaking antioxidant[8,9] and it is probably the most efficient antioxidant in the lipid phase.[10] In fact, more than 135 experimental and epidemiological studies (data retrieved from www.clinicaltrials.gov, October 2022) uphold a protective effect of VitE in several and diverse pathological processes, such as diabetes mellitus, metabolic syndrome, male infertility, cataract, cardiovascular disease, cystic fibrosis, neuro-degenerative diseases and cancer.[9,11] Furthermore, due to its high antioxidant and photo-aging protecting activity,[12,13] VitE is widely used in skin formulations, being applied in several cosmetics. Finally, the anti-inflammatory effect of VitE has been widely demonstrated.[14,15] Kuriyama and collaborators[16] have shown that a Vitamin E-based ointment is able to reduce chemically induced inflammation in rat keratinocytes.

The use of Vitamin E as an antioxidant has several important limitations such as instability due to pH changes, the possibility of having prooxidant effects at relatively low concentrations, and low aqueous solubility. Moreover, the formulation in organic solvents is needed.[17]

Being a lipophilic active compound, the bioavailability of VitE can be increased if associated with nanosystems such as nanostructured carriers, liposomes and nanoemulsions (NEs), promising alternatives to conventional formulations.[18,19]

In particular, NEs are colloidal systems stabilized by surfactants or surfactant mixtures.[20] The excipients used in NEs formulation are generally biocompatible and biodegradable. Oil-in-water (O/W) NEs have been proposed for drug and cosmetic formulations, notably for lipophilic molecules that can be incorporated and protected in the nanodroplets of the

inner oil phase.[21] The oily phase can consist of vegetable oils, which are rich in antioxidants along with unsaturated fatty acids, phytosterols and vitamins, contributing to the development and maintenance of health and well-being.[22,23]

The aim of this study was to prepare and compare functional O/W NEs loaded with VitE. Almond oil or Neem oil were employed to formulate NEs specifically for the purpose to enhance the biological effect of VitE. The composition of both oils is well known and reported in several studies.[24,25]

Neem oil from the seeds of *Azadirachta indica A. Juss* is rich in numerous bioactive phytochemicals, which are known to have excellent therapeutic potentials. Several studies demonstrated that these bioactive compounds display different effects on several biological processes such as inflammation, apoptosis, angiogenesis, and immunomodulation. In particular, a study based on HPLC analysis has revealed that neem oil contains phenolic compounds such as caffeic acid, vanillin, p-coumaric acid, vitamin D, vitamin E, and limonoids responsible for its antioxidant activity.[26] Moreover, in our previous work, the antioxidant activity of Neem oil NEs has been reported, confirming its biological effect also when the oil is structured in a nanoemulsion.[27] Among its numerous properties, Neem oil also has anti-inflammatory activity, thus being used in diseases involving an inflammatory state of the skin[28] thanks to components like nimbidin,[29] sodium nimbidinate,[30] polysaccharides, gallic acid, catechin and (-)-epicatechin.[31] Besides, Neem extracts can significantly reduce the release of proinflammatory cytokines and elevate the count of CD4+ and CD8+ T-cells.

The ability of Neem oil to scavenge free radicals and reduce ROS-mediated damage to cells has been demonstrated. Neem oil can be used to normalize lipid peroxidation and minimize ROS-mediated cell death.[32]

The use of this oil in pharmaceutical formulations is particularly favourable not only for its several biological effects but also for not showing hemolytic activity.[33]

Almond oil is rich in fatty acids, proteins, and carbohydrates. Moreover, it owns high number of vitamins and minerals, which make almond oil used widespread in medical applications for health benefits. In particular, the vitamin B complex and zinc content support and maintain the skin in healthy condition. Since the Almond oil is also a rich source of antioxidants, oleic acid (64–82%)[25] and VitE (240–440 µg/g),[34] avoiding the cell damage from free radicals and favoring their survival and growth.[35,36] Moreover, this oil shows low toxicity and blood compatibility,[36] making it a good component for pharmaceutical formulations.

The association of Vitamin E with other antioxidants has been proven to provide excellent skin protection,[37] and VitE-loaded NEs for dermal application have been formulated.[9,38]

According to aforementioned oil features, in this work, the potential synergy of the antioxidant activity of used oils and loaded vitamin E co-formulated in NEs have been explored by using three different models. For the in vitro experiments, keratinocyte cells are employed together with fibroblasts and melanocytes because they are the main cell-types in human skin. In particular, nontumorigenic HaCaT cells are a spontaneously immortalized, human keratinocyte line that has been widely used for studies of skin biology, differentiation and oxidative stress.[39–42] Instead, for the in vivo experiments, the nematode *Caenorhabditis elegans* (*C. elegans*) is used because in recent years it has emerged as a good in vivo model to study oxidative stress responses, including the ease of handling and the availability of transgenic animals. Indeed, using GFP-transgenic nematodes, fluorescence analysis of in vivo stress can be performed and the expression of genes encoding ROS detoxifying enzymes might be analyzed.[43] Finally, skin tolerability and anti-inflammatory activity were also evaluated in the final target, by performing in vivo experiments with healthy human volunteers.

Materials and Methods
Materials

Almond oil was purchased by Farmalabor Srl (Assago (MI) Italy). Neem oil was purchased by Neem Italia (Moniga del Garda (BS), Italy) and characterized by an ECOCERT certificate (Biocert Italia IT013BC041 – ICEA 264BC001). Polysorbate 80 (Tw80), tocopherol (vitamin E), Hepes salt {N-(2-hydroxyethyl), piperazine-N-(2-ethanesulfonic acid)}, 1.6-Diphenyl-1,3,5-hexatriene (DPH) and pyrene were Sigma-Aldrich products (Sigma-Aldrich, Milan, Italy). Ethanol and all other products and reagents were of analytical grade.

Pseudoternary Phase Diagram Construction

Pseudoternary phase diagrams were drawn in order to determine the region of existence of homogeneous O/W NE formulation. Several mixtures were prepared by combining appropriate amounts of surfactant, oil phase and aqueous phase (Hepes buffer 10^{-2} M, pH 7.4) in different weight ratios (Tables 1S and 2S), in a test tube and vortexed vigorously for 5 min to ensure thorough mixing. Each sample was visually inspected: when a clear and transparent sample was obtained after stirring, the sample was considered monophasic, in absence of phase separation, so pertinent to the NEs region.

Nanoemulsion Preparation

In order to select the region of existence of homogeneous O/W NE formulation, pseudoternary phase diagrams were drawn. Excess-water (O/W) nanoemulsions (NEs) (~95% water content) were prepared using Tw80 and Almond oil or Neem oil in different weight ratios. Tw80 concentration in the samples was always remarkably above CMC in water, at 20°C (0.012 mM).

Vitamin E was added to NEs at the maximum concentration solubilized by the oil phase and in the range of therapeutic doses, in accordance with commercial products (VitE at 5% w/v).

The NEs were obtained in Hepes buffer (pH 7.4 10^{-2} M) through a simple preparation method:[44,45] for each sample, all the proper components were vortexed for about 5 min and then 5 mL of Hepes buffer was added, thus obtaining an emulsion, with microscale droplets. Each emulsion was then sonicated for 20 min at 50°C, using a tapered microtip operating at 20 kHz at an amplitude of 18% (Vibracell-VCX 400, Sonics, Taunton, MA) to obtain NEs and VitE-NEs (Vitamin E loaded nanoemulsion). Different formulations are listed in Table 1.

Dynamic Light Scattering Measurements

Dynamic light scattering (DLS) analyses were performed with a Malvern Zetasizer Nano ZS90 (Malvern Instruments Ltd., Worcestershire, United Kingdom) to assess the size and the ζ-potential of the NEs and VitE-NEs. Obtained data represent average ζ-potential (mV) and hydrodynamic diameter (nm) of the NE droplets. The polydispersity index (PDI) value was also determined as an evaluation of the breadth of the size distribution.

Transmission Electron Microscopy

Morphological features of NEs were investigated by transmission electron microscopy (TEM). Diluted NE samples were adsorbed onto carbon-coated copper grids and negatively stained with 2% filtered aqueous sodium phosphotungstate

Table 1 Sample Composition[a,b]

Sample	Neem oil (mg/mL)	Almond oil (mg/mL)	Tween 80 (mg/mL)	Vitamin E (mg/mL)
N[c]/N1	**19.6**	–	**29.6**	**–**
N1E				**50.0**
N2	19.6	–	39.2	–
N2E				50.0
A[c]/A1	–	**19.6**	**19.6**	**–**
A1E				**50.0**
A2	–	19.6	29.6	–
A2E				50.0

Notes: [a]All tested formulations have a pH between 5.0 and 5.5 (Detailed method to measure pH was included in Supplementary Materials). [b]Compositions in bold correspond to the NEs selected for in vitro and in vivo experiments. [c]Samples N and A are the same as N1 and A1, before sonication.

adjusted to pH 7.0. The excess staining solution was then drained with filter paper, and preparations were observed with a transmission electron microscope (EM 208, FEI Company, Eindhoven, The Netherlands) at an accelerating voltage of 80 kV.

Small Angle X-Ray Scattering (SAXS) Measurements

SAXS experiments were carried out at the European Synchrotron Radiation Facility (ESRF, Grenoble, France), beamline ID02, in the region of momentum transfer $0.017nm^{-1} \leq q \leq 5nm^{-1}$, $q = (4\pi/\lambda) \sin(\theta/2)$, being θ the scattering angle and λ the incident wavelength ($\lambda = 0.995$ Å). Polycarbonate capillaries of 2 mm thickness (ENKI, Concesio, Italy) were used as sample cells. The measured 2D SAXS patterns were submitted to standard correction and normalization procedures, then angularly regrouped to obtain the intensity profile I(q) as a function of q. The background signal was subtracted from the average spectrum (n = 5) of each sample, after excluding any possible radiation damage. The intensity decay behavior as a function of momentum transfer q, I(q), can provide details on the internal structure of NEs in solution down to the nm length-scale.

The best fits to the intensity profiles for the measured NEs were obtained using either a model consisting of globular clusters with fractal internal arrangement, mass fractals, or a model of hierarchical fractal aggregates with two different fractal dimensions. Spectra have been reconstructed with SasView application.[46,47]

Oil Nanodroplet Characterization

The spatially sensitive fluorescent Pyrene probe was included in the formulation to highlight the effect of surfactant present at oil/water interface on the oil droplet features.

Pyrene loaded samples were prepared by adding pyrene (4 mM) with other lipophilic components (same preparation method as above) and fluorescence experiments were carried out following the signals emitted by pyrene-loaded samples evaluating its emission spectrum ($\lambda = 350–550$ nm, Ex = 330 nm). The pyrene probe, entrapped mainly in the lipophilic portion of NEs and VitE-NEs, allows us to investigate the lateral distribution and the dynamics of oil drop (oil and surfactant chains). Pyrene is a spatially sensitive probe and displays an ensemble of monomeric fluorescence emission peaks in the range from 375 to 405 nm and a band around 460 nm related to the formation of an excimer (two monomers spatially proximal).[48,49]

pH Evaluation

All formulations were tested to have a suitable pH for topic administration (4 < pH < 7) by pH-meter Hanna instrument (HI 2211 pH/ORP meter). All tested formulations have a pH between 5.0 and 5.5, stable for at least 3 months, in the range typical of healthy skin (pH 5.0–6.5).

Physicochemical Stability

Specific studies on physical stability of NEs and VitE-NEs, composed by Tw80 and either Almond or Neem oil at different ratios, were carried out to investigate whether significant size and ζ-potential changes in NE dispersion occur during storage at the two selected temperatures, using Hepes buffer as aqueous phase. The NEs were stored at 4 and 25°C for 3 months. Samples were analysed at definite time intervals (1, 30, 60 and 90 days) and the ζ-potential and the average hydrodynamic diameter of NEs were measured as previously described. In addition, the UV spectra of NEs were recorded immediately after sample preparation and after 90 days to evaluate Vitamin E stability against decomposition/degradation.

In vitro Release Studies

The experiments were carried out using dialysis tubes (MW cut-off 8000 and 5.5 cm^2 diffusing area) at 32°C. The set-up was kept at T = 32°C by means of a temperature-controlled water bath, and the release medium (Hepes: EtOH 96° 80:20) was submitted to gentle stirring during the experiment. Sample aliquots (1 mL) were withdrawn from the release medium solution at specific time intervals during 24 h for UV analyses and then reinserted back. Released Vitamin E was detected by means of a spectrophotometer (Perkin-Elmer, lambda 3a, UV–vis spectrometer). Aliquots were analyzed immediately after sampling. All release experiments were carried out in triplicate, and individual results lay within 10% of the reported mean values.

Cell Line and Cell Culture

Normal human keratinocytes (HaCaT), purchased from Thermo Fisher Scientific (Thermo Fisher Scientific, Waltham, MA, USA), were maintained in a humidified atmosphere of 5% CO2 at 37°C in Dulbecco's Modified Eagle Medium (DMEM, Corning Manassas VA, US) supplemented with 10% heat-inactivated fetal calf serum (FCS, Euroclone, Italy) and 1% penicillin-streptomycin (Sigma-Aldrich, St. Louis, MO, USA) and 1% L-glutamine (Sigma-Aldrich, St. Louis, MO, USA).

Cytotoxicity Assay (MTT)

The cell metabolism of HaCaT cells was measured by MTT (3-(4,5-dimethylthiazol-2-yl)-2,5-diphenyltetrazolium bromide) assay. The MTT assay uses the ability of the mitochondrial succinate dehydrogenase enzyme to convert the yellow salt of MTT to the purple formazan crystalline which is insoluble in water. After the addition of dimethyl sulphoxide (DMSO) as solvent, formazan is solved, and the produced color is measured at the specified wavelength by using a microplate reader. Briefly, 96-well plates were seeded with $3X10^5$/mL HaCaT cells, and, after 48 h of incubation, monolayers were treated with different NE concentrations ranging from 5.0 to 0.005 mg/mL of surfactant (Tw80). After 24h, the medium was removed, the cells were washed with phosphate-buffered saline (PBS) and, subsequently, incubated with 0.5 mg/mL MTT (Sigma-Aldrich, St. Louis, MO, USA) for additional 4 h. Finally, the medium was removed, the cells were washed with PBS for three times, and then, 100 μL of DMSO (Sigma-Aldrich, St. Louis, MO, USA) was added to dissolve the formazan crystals. Optical density (OD) at 570 nm was determined with a spectrophotometer/ fluorimeter microplate reader (PerkinElmer, Hopkinton, MA), and the cell viability for each concentration was estimated through comparison with untreated cells. HaCaT cells cultured in DMEM without the addition of compounds were used as a control. Ten percent of DMSO was used as positive control.

C. elegans Lifespan and Fluorescence Analysis

The *C. elegans* strains used in this study were the Bristol wild type N2 and the CF1553 (muls84[pAD76(Sod-3::GFP)]) transgenic strain, from Caenorhabditis Genetic Center.[50]

The two strains were grown at 16°C on Nematode growth medium (NGM) plates with fresh *Escherichia coli* OP50 as standard laboratory food. For lifespan assay, *E. coli* OP50 cultures were prepared by inoculating a single colony in 50 mL of Luria Bertani (LB) broth and incubated at 37°C overnight, under shaking. Overnight cultures were then incubated at 65°C for 90 min and deposited onto NGM agar plates. Heat-killed cells were also plated on LB agar in parallel to ensure that no viable cells remained. Bacterial lawns used for *C. elegans* lifespan assays were prepared by spreading 60 μL of heat killed *E. coli* OP50 on the NGM agar plates (35 mm). For each condition, 60 μL of different nanoemulsions (A1E, A1, N1E, N1 and respective 1:5 or 1:1 dilution in Hepes buffer) were also spotted onto the plates before seeding worms. Worms fed with *E. coli* OP50 without nanoemulsion supplementation were used as control. For fluorescence microscopy analysis, nematodes prepared as described above, at the stage of 2-days adult were mounted onto 3% agarose pads according to Schifano et al, 2019.[51] Quantification of fluorescence intensity was evaluated with Image J 1.43 (NIH) software. For each sample, 10 transgenic nematodes were analyzed and the mean value was reported.

In vivo Skin Tolerability Test and Anti-Inflammatory Activity of the Formulations

In vivo investigation was further extended to test a possible skin application of NEs. To this end, in vivo experiments were performed on healthy human volunteers to assess skin tolerability and anti-inflammatory activity of NEs by using the reflectance spectrophotometer, SP60 (X-Rite Incorporated, USA) connected to a personal computer. This tool allows in vivo analysis by a non-invasive technique. The spectrophotometer was operated with 0° illumination-angle and 45° viewing-angle and it was calibrated before any experiment, with the provided white-standard referable to the National Bureau of Standard's perfect white diffuser. Appropriate data analysis was allowed to perform colorimetric evaluations from the spectral data. An illuminant C and 2° standard observer were used to visualize the reflectance spectra over the wavelength range 400–700 nm. Eight healthy volunteers, after being informed on the nature of the experimental study, signed a detailed informed consent. The volunteers involved in the study had no disease, did not present dyschromia on

the skin surface used for the tests, and did not take drugs for at least one week before the experiment. They rested for 30 minutes in the place where the experiment was carried out to acclimatize at room condition ($25 \pm 3°C$ and $40 \pm 50\%$ relative humidity).

To study the tolerability of formulations, nine sites (one for the saline solution and two for each sample), each of 1 cm^2, 2 cm far from each other to avoid interferences, were defined on the ventral part of each forearm of the eight healthy human volunteers. Before the application of the samples, Erythema index (EI) baseline values of each site were measured. Then, Hill Top Chambers (Hill Top Research, Inc. Cincinnati, Ohio) were used for the application of samples N1, N1E, A1 and A1E. Saline solution (NaCl 0.9% w/v) was used as control. Before X-Rite measurement of the possible induced erythema (EI), Hill Top Chambers were removed, and the surface of the skin was left to dry for 15 minutes after being gently washed with water to remove any formulation residues. Analyses were performed at 6, 24, 48 hours after sample application, and the possible induced erythema (EI) was calculated through the following equation:

$$EI = 100[log1/R_{560} + 1.5(log1/R_{540} + log1/R_{580}) - 2(log1/R_{510} + log1/R_{610})] \qquad (1)$$

where 1/R is the inverse reflectance at a specific wavelength (510, 540, 560, 580, 610).[52]

The in vivo tests were performed in accordance with the Declaration of Helsinki, and the protocol was approved by the Research Ethics Committee of the University of Catanzaro "Magna Græcia" (Approval number: 392/2019).

The anti-inflammatory activity of the tested formulations in vivo was evaluated by measuring the reduction of the skin erythema induced by the application of a skin chemical irritant (methyl-nicotinate) compared with a saline solution. Nine sites (one for the saline solution and two for each sample), each of 1 cm^2, at a distance of 2 cm from each other, were randomly defined on the ventral part of the forearm of eight volunteers; then, 100 µL of an aqueous methyl-nicotinate solution (0.2% w/v) was applied using Hill Top Chambers on each site. After 15 minutes, the chambers were removed and the skin was gently cleaned with water to eliminate methyl-nicotinate solution residues; then 200 µL of each formulation (N1, N1E, A1, A1E) were applied, each on a different site. One of the defined site (control) was treated with 200 µL of saline solution (NaCl 0.9% w/v), used as control of the physiological skin recovery. Before carrying out any analysis with X-Rite at established time, the chambers were removed, the surface of the skin cleaned with water and left to dry for 15 minutes. The spectrophotometric measurements were carried out every hour until the disappearance of the chemically induced erythema, starting from 1h from NE (or buffer) application. For each delay, the $\Delta EI(t)$ was calculated as: $\Delta EI(t) = EI(t) - EI(baseline)$. The in vivo tests were performed in accordance with the Declaration of Helsinki, and the protocol was approved by the Research Ethics Committee of the University of Catanzaro "Magna Græcia" (Approval number: 391/2019).

Data Analysis and Statistics

All experiments were performed at least in triplicate. Data were presented as mean ± SD. For the cytotoxicity assay, the ANOVA test followed by Tukey's post hoc pairwise tests has been performed. Computed p values have been corrected by using the Benjamini–Hochberg procedure in order to take into account multiple comparisons. For C. *elegans* lifespan, statistical analysis was performed Kaplan–Meier survival plot coupled with Log-rank (Mantel-Cox) test. For oxidative stress, statistics was performed by one-way ANOVA coupled with Bonferroni post-test (GraphPad Prism 5.0 software, GraphPad Software Inc., La Jolla, CA, USA). Also, for in vivo studies, statistical analysis was performed with the ANOVA test, and Bonferroni t-test was used for comparison between sites treated with formulation and control (sites treated with saline solution). Differences with p values <0.05 were considered significant and were indicated as follows: *p < 0.05, **p < 0.01, and ***p < 0.001.

Results and Discussion
NE Physical-Chemical Characterization

The choice of surfactant is crucial to obtain emulsified systems, thereby influencing their physicochemical properties. As a rule of thumb, surfactants with an HLB (hydrophilic–lipophilic balance) value around 15 are considered to be able to produce a homogeneously dispersed phase with small droplet size distribution and uniformity over a wide domain of relative composition of constituents.[53]

The nonionic Tween 80 (HLB = 15) was chosen as stabilizing agent because of its efficacy in lowering the interfacial tension, its suitability for oil-in-water emulsions as compared to ionic surfactants[54] and its ability to form smaller droplets.[55] Tween 80 is also less distressed by ionic strength and pH.[56] Furthermore, NEs prepared with Tween 80 have been described to display long-term stability (180 days),[57] as their large hydrophilic head group prevents droplet aggregation by electrostatic and steric repulsion.[58] Finally, Tween 80 is widely used as a solubilizing agent in commercial products such as creams, ointments, lotions and emulsions,[59] showing biocompatibility and safety.

Since the surfactant and oil composition strongly influence the NE stability, the ternary surfactant/oil/water phase diagrams were assessed for the Neem-based and the Almond-based systems. The homogeneous nanoemulsion phase regions were identified, to select the appropriate NEs in terms of hydrodynamic diameter, ζ-potential, and polydispersity index (PDI). In Figures 2S and 3S, the phase diagrams of the ternary Tween 80 – Hepes – vegetal oil (either Almond or Neem) are shown, evidencing the domains of homogeneous dispersions against the non-homogeneous ones, character-ized by phase separation. We observed that occasionally monophasic dispersions could be obtained after sonication of some formulations belonging to non-homogeneous regions. According to that observation, also samples belonging to the monophasic emulsions phase region were sonicated to optimize homogeneity. Two formulations were selected for both Almond-based (A1 and A2) and Neem-based (N1 and N2) systems, as listed in Table 1, belonging to the water-rich homogeneous region, showing best values of hydrodynamic diameter, ζ-Potential and PDI, candidates for VitE loading (A1E and A2E; N1E and N2E). Although showing similar values of hydrodynamic diameter and ζ-potential values (Tables 2 and 3S), samples A1 and A1E, N1 and N1E were considered for further characterization. In fact, the lowest amount of surfactant (approximately 4–10 wt%) was chosen to minimize toxicity problems, and the highest oil content was chosen as a prominent criterium, to focus on the potential adjuvant effect of the oil on Vitamin E, loaded at the same concentration, for in vitro/in vivo studies.

As a general rule, the size of the disperse-phase droplets gets smaller as the concentration of surfactant increases.[44] Sample A1, with the lowest Tween 80 concentration was found to display the highest hydrodynamic diameter (Tables 2 and 3S). NE composition and NE preparation allowed to obtain a hydrodynamic diameter of about 100 nm without using a mixture of surfactants with different HLB[60] or ethanol, as co-surfactant.[61]

In Neem-based NEs (sample N1 and N2, Table 3S), the nanodroplet size was not affected by the amount of surfactant, seemingly being the fraction of surfactant high enough to stabilize Neem oil small droplets.

Besides the extension of the disperse-droplets monophasic region, the oil component affects many nanodroplets features, size, morphology, internal structure, and core fluidity.

NE Morphology

To visualize morphological aspects, NE formulations were observed by TEM. Before sonication, the ultrastructural characteristics of the NEs showed non-homogeneous feature, with objects of different size and shape. In particular, the A sample (Figure 1A) showed polydisperse droplets, different in morphology and size, whereas the N sample (Figure 1D)

Table 2 Sample Characterization

Sample	Hydrodynamic Diameter (nm) ± SD	ζ-Potential (mV) ± SD	PDI
N[a]	808.80 ± 11.6	−32.8 ± 1.0	0.3
N1	73.4 ± 7.6	−16.2 ± 0.5	0.4
N1E	174.2 ± 8.4	−11.1 ± 0.2	0.2
A[a]	202.0 ± 10.8	−17.0 ± 0.6	0.3
A1	114.1 ± 3.8	−6.8 ± 0.2	0.4
A1E	266.2 ± 7.1	−10.1 ± 0.5	0.2

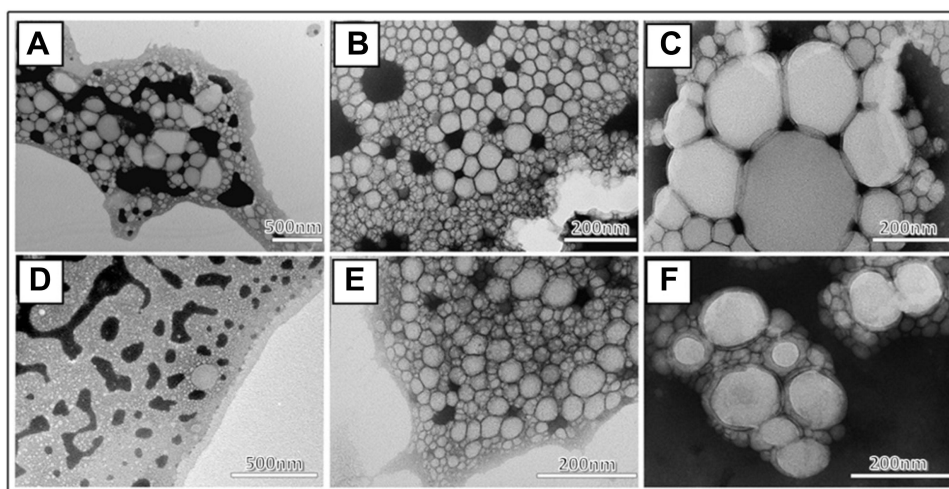**Note**: [a]Samples N and A are the same as N1 and A1, before sonication.

Figure 1 Morphological observations of nanoemulsions by transmission electron microscopy. Upper row: Almond-based NEs; bottom row: Neem-based NEs. (**A** and **D**): NEs before sonication (samples A and N); (**B** and **E**): Empty NEs after sonication (samples A1 and N1); (**C** and **F**): Vit-E loaded NEs (samples A1E and N1E).

appeared as containing an irregular network and small droplets. After sonication (samples A1 and N1), almost spherical droplets of different sizes were seen (Figure 1B and E) in both systems. A1 nanoemulsions appeared more regular in shape and size, as compared to N1 samples, and showed a more ordered spatial arrangement of the droplets. In both samples, many particles showed a non-uniform structure, with internal inhomogeneity, as if small droplets were tightly clustered into larger drops. Finally, when loaded with vitamin E, NEs particles became larger in size, still spherical in shape (Figure 1C and F). All samples looked polydisperse, with larger sizes corresponding to those revealed by DLS analysis.

NE Structure

The structure of NEs was investigated by SAXS. The intensity spectrum of Neem-based NEs (N1) is reported in Figure 2A (grey dots) in log–log scale, showing a plateau at low q values and a quite monotonous decay at high q values. This behaviour reveals the presence of particles with nanometric size. The intensity profile has been modelled to globular particles, with average size 20 nm, with a non-uniform internal structure, characterized by a mass fractal dimension 2.4, $I(q) \div q^{-2.4}$. The intensity spectrum of Almond-based NEs (A1) reported in Figure 2B (orange dots) displays two distinct power-law decays. In the high-q region $I(q) \div q^{-2.1}$, while in the low-q region $I(q) \div q^{-1.5}$. This behaviour suggests a hierarchical
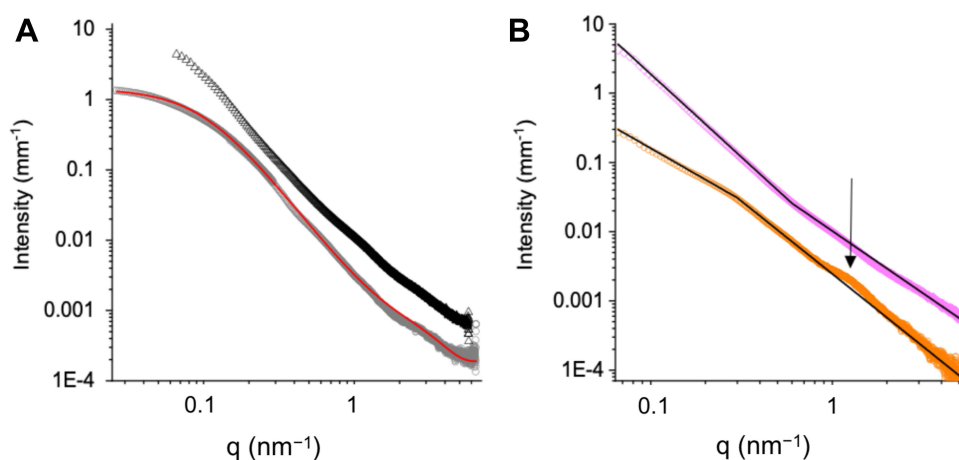

Figure 2 SAXS profiles of NEs. (**A**) Neem-based NEs intensity profiles: unloaded N1 (gray dots), VitE-loaded N1E (black triangles) in log-log scale. (**B**) Almond-based NEs intensity profiles: unloaded A1 (Orange dots), VitE-loaded A1E (magenta diamonds) in log-log scale. Solid lines are the best fits for the form factors of the particles.

arrangement of primary particles, with inhomogeneous internal structure, in fractal branched clusters, ordered on a longer length-scale as compared to Neem-based NEs. Also, on the local scale, the presence of a broad peak at q = 1.2 nm^{-1} indicates that the internal inhomogeneity has a characteristic distance d = 2π/q = 5.2 nm. This length is of the order of twice the length of a polysorbate 80 molecule. The oil component can be solubilized within the oleic acid chains.

Structural results on NEs correlate with the morphology presented in Figure 1B and E. Both Neem-based and Almond-based NEs show the presence of small droplets, clustered in larger drops. The Almond-based system presents a higher degree of order on both the local and the cluster length-scale.

The intensity profiles of VitE-loaded NEs are reported in Figure 2, upper data, for Neem-based (black triangles, Panel a) and Almond-based NEs (magenta diamonds, Panel b). Differences from the intensity profiles pertinent to the corresponding unloaded NEs are visible both in the scattered intensity and in the trend in the low-q region. For Almond-based formulation, the higher intensity at low-q and the steeper slope, I(q) ÷ q$^{-2.4}$ (magenta diamonds), instead of I(q) ÷ q$^{-1.5}$ (orange dots) indicates the presence of more compact larger drops. For Neem-based formulation, the trend in the low-q region indicates the formation of larger drops (black triangles), although less coordinated with respect to Almond-based ones. The observed increase in size for both systems is consistent with DLS and TEM results. In the images (Figure 1B and C) the higher propensity of Almond-based droplets to regular arrangement and coordination agrees with the scattering results relative to the formulation as a whole. The addition of Vitamin E modifies the hydrophobic/hydrophilic balance, increasing the hydrophobic volume fraction with respect to the hydrophilic one, thus favouring the formation and stabilization of larger oil droplets.

Oil Nanodroplet Characterization

Fluorescence spectra (Figure 3) indicate that in Neem-oil nanodroplets, Pyrene is present in the excimer form, suggesting a low probe "mobility"; these data are consistent with the fluorescence anisotropy value of 0.34, also suggesting that Neem nanodroplet fluidity is low.[62] Similar results are obtained for both unloaded NEs and loaded with Vitamin E (N1 – N1E), in agreement with the N1E internal structure, as revealed by SAXS. In fact, the internal hydrophobic core of Neem oil nanodroplets enlarges to host VitE, still keeping the globular shape.

Reversely, in the Almond oil nano-droplets, Pyrene is present both as monomer and as excimer, suggesting higher fluidity, again confirmed by the fluorescence anisotropy value (0.1). The intensity of the excimer peak is decreased upon addition of Vitamin E, outlining an alteration of the organization of the dispersed system.

Still, these results do not match the mere oil-phase properties. In fact, Neem oil has lower viscosity (about 0.2 poise at 25°C) than Almond oil (about 0.4 poise at 25°C). Their density and surface tension are similar (about 0.9 g/cm^3 and 8 dyne/cm, respectively).[48] It has been noted that the features displayed by dispersed nanodroplets may be a result of different surfactant distributions at oil/water interface.[63] Here, the difference in the structural arrangement on the local-scale (Figure 2) can explain the different fluidity observed by Pyrene. The probe could diffuse for longer distances in the Almond oil droplets that display a regular internal packing, likely a double layer with a hydrophobic core.

Stability Studies

Stability studies on unloaded and loaded NEs were carried out over a period of three months. The unloaded samples of both NEs were kept at 4°C and 25°C. For Vitamin E-loaded samples, instead, only storage at 25°C was considered, as at 4°C the viscosity of the systems soon exceeded the value suitable for DLS analysis.

As shown in Figure 4A, the average hydrodynamic diameter and ζ-potential of all tested samples are stable for at least 90 days, with no significant variation.

In addition, to assess whether any degradation phenomena affect Vitamin E after inclusion in the oil dispersed phase of NEs, the UV spectra were recorded immediately after sample preparation and after 90 days and compared to free VitE. As reported in Figure 4B, the recorded values are superimposable, showing that inclusion of Vitamin E in NEs does not affect its stability.[64]
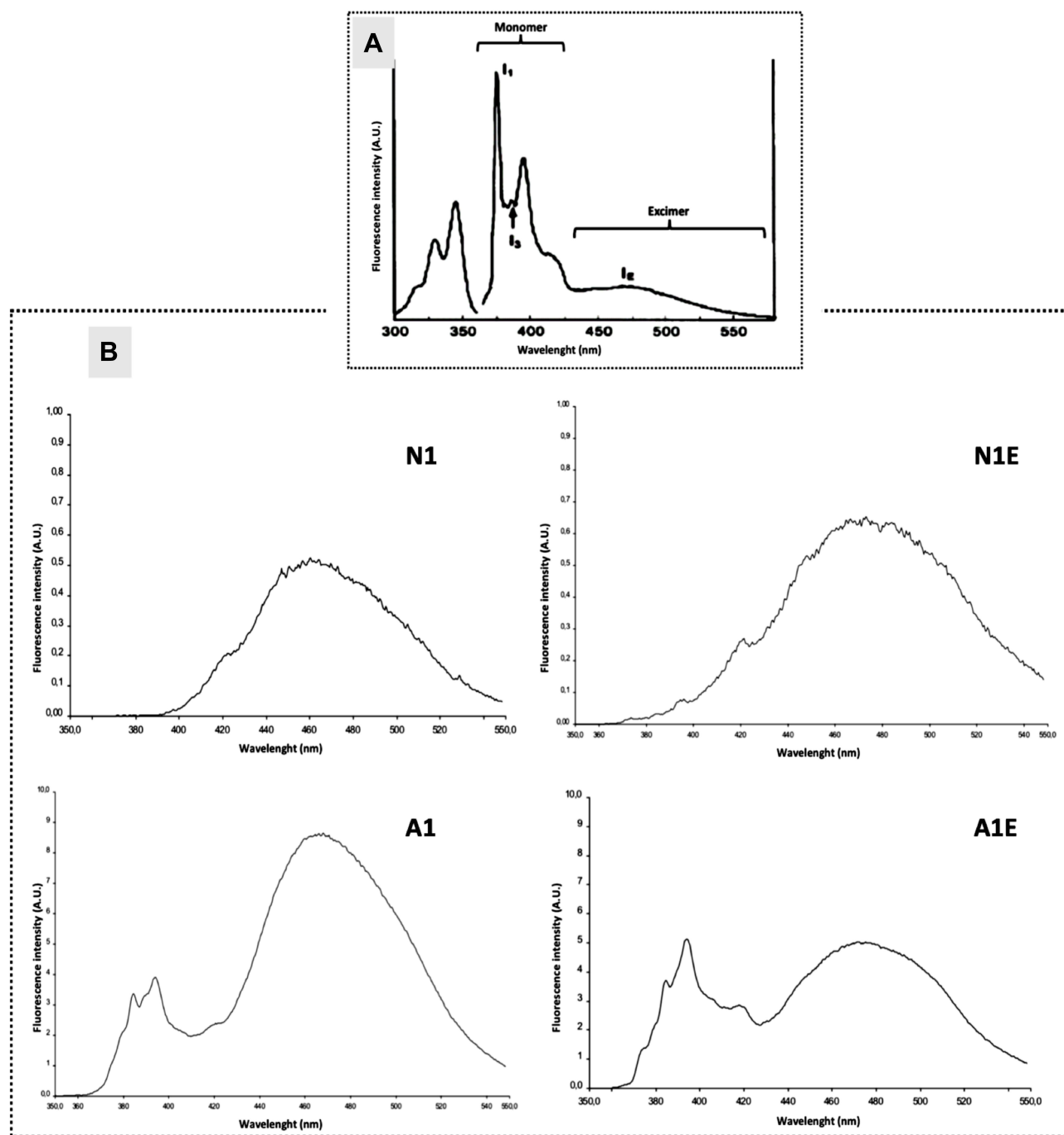
Figure 3 Pyrene spectra. (**A**) Fluorescence emission spectrum of pyrene. (**B**) sample spectra.

In vitro Release of Vitamin E

The release of Vitamin E by NEs was estimated by diffusion studies at T = 32°C, similar to skin surface, during 24h. As shown in Figure 4S, approximately 40% of the Vitamin E content was released after 24 hours, mostly within the first 9 hours (30–35%), in agreement with data recorded for water-rich O/W nanoemulsion obtained by α-tocopherol/deionized water.[65] Both Almond-based and Neem-based formulations displayed the same release profile, despite the chemical-physical difference in oil nanodroplets. This could be explained by considering that the two systems have similar nature once in the presence of Vitamin E, as evidenced by SAXS results.
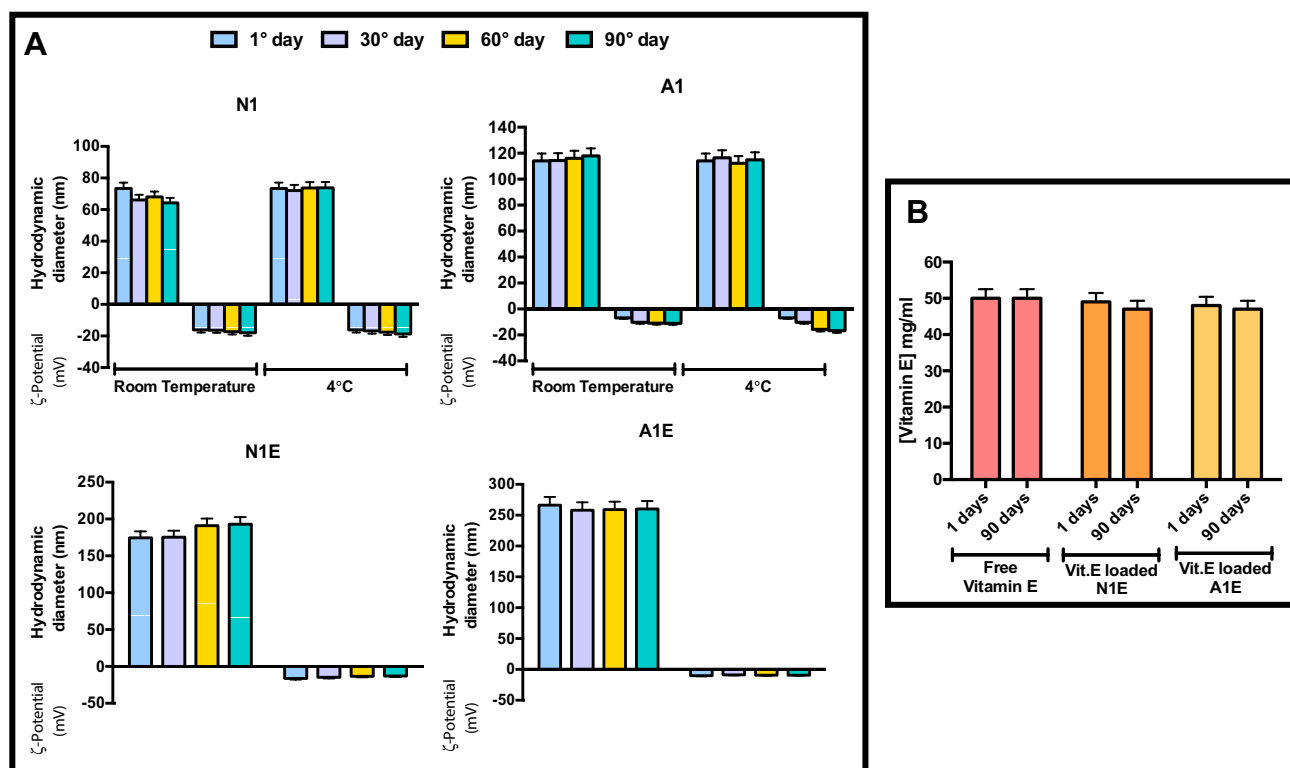
Figure 4 Time stability of NEs size and charge. (**A**): Top row: unloaded NEs; bottom row: VitE-loaded NEs. Left column: Neem-based NEs; right column: Almond-based NEs. (**B**) Chemical time stability of Vitamin E loaded in NEs as compared to free VitE, up to 90 days at room temperature.
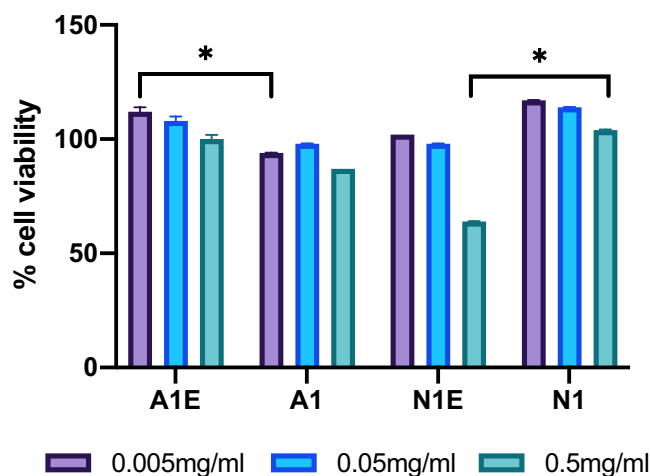

Figure 5 Cell viability of human keratinocytes after A1E, A1, N1E or N1 nanoemulsions exposure. HaCaT cells were pretreated with various concentrations (respect to surfactant) of NEs for 24 h. Data are reported as percentages of the control. Data are expressed as means ± standard deviations from at least three independent experiments performed in triplicate. Asterisks indicate statistically significant differences at $p \leq 0.01$.

Effect of NEs on Cellular Viability

Cell viability after exposure to NEs was estimated on keratinocytes, after 24 h incubation with different concentrations of A1E, A1, N1E or N1, by MTT assay. As shown in Figure 5, no cytotoxic effect was induced by unloaded A1 and N1 formulations.

As reported by some authors, sensitivity to nanoemulsion treatment was cell dependent.[66] Mericli et al, 2017[67] demonstrated that Almond oil, rich in oleic acid, was able to inhibit the growth of colon cancer cells in a dose- and time-dependent manner. On the other hand, differently to that previously observed for HEp-2 cells,[27] in which a low toxic effect was correlated with oil/surfactant NE incubation, N1 formulation did not influence keratinocyte vitality.

In our study, statistically significant differences in cell viability have been observed among formulations (ANOVA F 71.6 p value <0.0001). A more evident and significant reduction of cell viability was observed after treatment of monolayers with higher concentration (0.5 mg/mL) of N1E with respect to N1. At 0.05 mg/mL concentration, only a slight but significant decrease in mitochondrial function of keratinocytes exposed to A1 was noticeable, but the nanoencapsulation of Vitamin E was able to protect against the reduction of cellular viability. In this research, the loading of vitamin E did not further enhance cell death when compared to unloaded nanoemulsion at the same dose, suggesting that the vitamin did not contribute to the reduced cell viability in HaCaT cells.

C. elegans Vitality

To compare the in vivo effects of the different NEs, *C. elegans* model system was used. The vitality of *C. elegans* either fed on heat-killed *E. coli* strains OP50 (control) or supplemented with A1E, A1, N1E and N1 was evaluated during 14 days. Lifespan assay showed that the different NEs did not exert toxic effects on *C. elegans* worms. In particular, nematodes treated with A1E or N1E showed a 50% vitality after 9 and 11 days, respectively, as compared to 8 days of the control population. On the other hand, 50% of worm viability in nematodes supplemented with A1 or N1 nanoemulsion was recorded at day 8, similarly to heat-killed OP50 fed worms (Table 3). In the case of nematodes supplemented with diluted NEs (1:5 or 1:1 dilutions), the lifespan was almost identical to the control (data not shown).

We also used *C. elegans* as an in vivo model system to test the antioxidant potential of the two NEs. Indeed, one of the roles played by antioxidant supplementation is the modulation of endogenous defenses, leading to a delay in aging. Vitamin E is considered to be the most established lipophilic antioxidant, affecting the lifespan and oxidative biomarkers in *Caenorhabditis elegans* under oxidative stress.[68] However, it has been reported that during the aging process, products of oxygen metabolism accumulate in tissues, damaging proteins, lipids and DNA, and weakening antioxidant defenses.[69] In *C. elegans*, several studies have been performed to better understand the mechanisms through which different signaling pathways relate longevity, aging, and oxidative stress resistance.[70–72] Some of these pathways lead to the expression of detoxifying enzymes, such as the superoxide dismutase SOD-3, normally induced in response to stress. Indeed, the sod-3 gene encodes the Fe/Mg SOD potentially resisting oxidative stress and promoting longevity.[73]

To analyze whether the different nanoemulsions could stimulate oxidative stress response in *C. elegans* model, fluorescence microscopy with the transgenic *C. elegans* sod-*3*::GFP strain was performed (Figure 6).

Interestingly, transgenic worms supplemented with A1E and A1 caused an increment in SOD-3 expression with respect to the control; the effects observed increased proportionally with increasing concentration of the different nanoemulsions (Figures 6A and 5S). In the case of undiluted samples, nematodes supplemented with A1E showed a reduced oxidative stress response compared to A1 treatment. On the other hand, N1E showed increased fluorescence compared to N1 nanoemulsions, when supplemented at higher concentrations, although the values are lower compared to that observed for the almond NEs (Figures 6B and 5S). According to our results, vitamin E reduced oxidative stress by increasing SOD-3 activity and promoting animal growth and health status.[74,75]

Table 3 Kaplan–Meier Survival Plot of N2 Worms Fed with Heat-Killed *E. coli* OP50 Supplemented with A1E, A1, N1E or N1 NEs. The Lifespan of Heat-Killed OP50-Fed Animals Was Reported as Control (-). Three Experiments Were Performed in Triplicate for Each Condition (Ns: Not Significant)

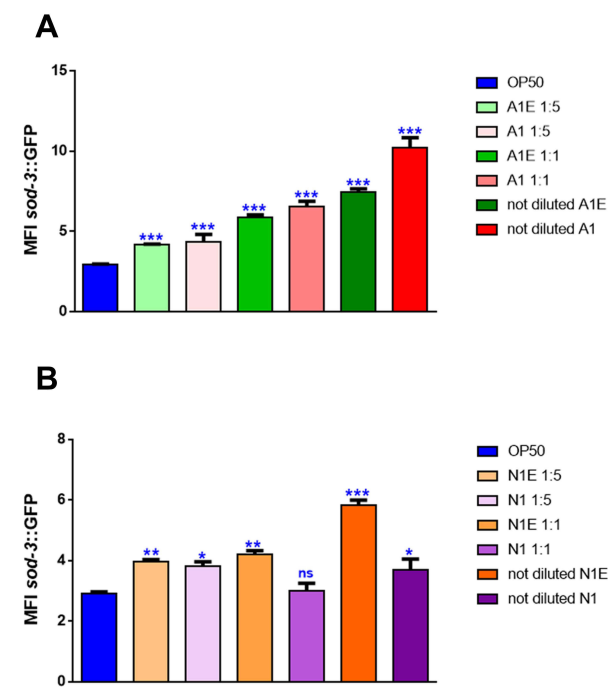| *C. elegans* Strain	Treatment	n	Median Lifespan	Maximum Lifespan	Number of Censored	Statistics
Wild-type N2	-	200	8 ± 0.8	8 ± 0.8	15	-
	A1E	200	9 ± 0.9	12 ± 0.4	12	p< 0.01
	N1E	200	11 ± 1.2	14 ± 0.8	18	p< 0.001
	A1	200	8 ± 0.2	12 ± 0.3	10	ns
	N1	200	8 ± 0.4	14 ± 0.9	12	ns

Figure 6 Analysis of oxidative stress responses in transgenic *sod-3*::GFP nematodes. Median fluorescence intensity of *sod-3*::GFP worm strain at the stage of 13 days adult fed heat killed OP50 (control) supplemented with (**A**) A1E, A1, (**B**) N1E and N1 nanoemulsions at different dilutions. Statistical analysis was evaluated by one-way ANOVA with the Bonferroni post-test; asterisks indicate significant differences (*p<0.01; **p<0.01; ***p<0.01). Bars represent the mean of three independent experiments.
Abbreviation: ns, not significant.

Skin Tolerability Test and Anti-Inflammatory Activity Results

Skin tolerability is a fundamental parameter to be evaluated for all formulations that could potentially be applied on the skin. To verify that the NEs do not cause irritation when topically applied on the human skin, reflectance spectrophotometric studies were performed on healthy human volunteers. As reported in Figure 7, none of the considered NEs led to significant variation of the erythema index (ΔEI) values compared to those obtained upon application of a saline solution (0.9% w/v NaCl) used as
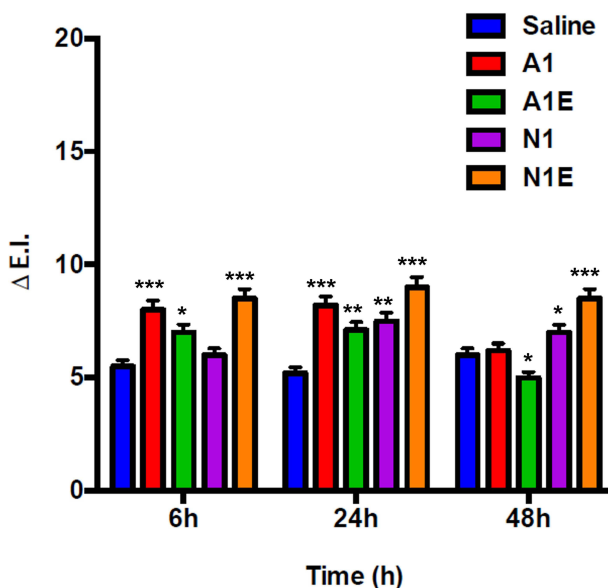

Figure 7 In vivo skin tolerability of the formulation expressed as variation of the erythema index (ΔEI). Results are the mean of three experiments ± standard deviation. Data obtained testing formulation A1, A1E, N1 and N1E were compared to the ones carried out by saline solution. *p < 0.05, **p < 0.01, and ***p < 0.001.

a control, at all explored delays. Thus, we can establish that all formulations are well tolerated when applied on the skin. In addition, also the anti-inflammatory activity of NEs, ie, their ability to reduce the erythema induced chemically, was evaluated on healthy human volunteers. Well-defined circular sites on the ventral part of the subjects' forearm were pretreated with an aqueous methyl-nicotinate solution (0.2% w/v) to induce erythema. Then, the NEs were applied, each on a specific site, and the erythema index (EI) was measured over 5 hours. As shown in Figure 8, ΔEI values remain high upon application of both Almond-based NEs (A1 and A1E) for all the duration of the experiment, with values similar to those recovered upon application of mere saline solution to the irritated skin, emphasizing the persistence of the induced erythema. Results show that Almond-based NEs, both unloaded or loaded with VitE, are not able to reduce the skin erythema induced by methyl nicotinate.

Reversely, application of Neem-based NEs (N1 and N1E) produced a pronounced decrease of ΔEI values. The anti-inflammatory property of Neem oil is well documented in literature,[76] then the ability of Neem-based NEs to reduce the chemically induced skin erythema was awaited. Nonetheless, the VitE supplemented NEs (N1E) showed the most pronounced ΔEI reduction power, that is, it was more efficient than its unloaded analogue, and it was able to restore the skin in the experiment time-course. This result stems for a synergistic effect, more than additive, in coupling the anti-inflammatory properties of vitamin E[14] and Neem oil in Neem-based NEs. As shown in Figure 8, ΔEI values relative to N-type NEs, are already much lower than the A-type analogues at 1h delay from application, indicating that the anti-irritant effect is prompt, besides efficient. It is interesting to notice that the synergistic effect as anti-irritant is not displayed by Almond-based NEs, despite the natural presence of VitE in Almond oil and of similar amounts of VitE in supplemented NEs. This result could be attributed to the chemical composition of two oils. According to the literature, the anti-inflammatory activity of neem oil is particularly notable and successfully observed in both acute and chronic inflammation.[76–78] Probably, for this reason, the NEs composed of Neem oil showed a higher synergistic anti-irritant effect. Furthermore, this effect of Neem-based NEs is not evident in in vitro studies or on *C. elegans* but only on human skin. This effect could be related to a higher skin penetration and retention propensity than the Almond formulations.[79] Few studies have been published on the comparison of the activity of oil constituents with penetration enhancement through the skin, thus further in vitro/in vivo studies need to be performed to confirm this mechanism.
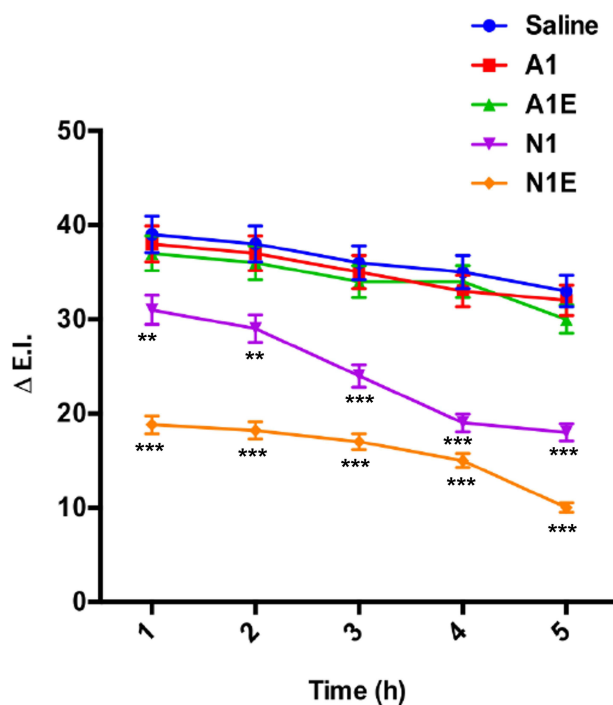

Figure 8 In vivo anti-inflammatory activity of formulations evaluated as their ability to reduce chemically induced skin erythema. Results are expressed as variation of the erythema index (ΔEI) and are the mean of three experiments ± standard deviation. Data obtained testing formulation A1, A1E, N1 and N1E were compared to the ones carried out by saline solution. **p < 0.01, and ***p < 0.001.

Conclusion

The golden thread of the present study was to assess whether Vitamin E shows enhanced antioxidant activity promoted by its formulation in NEs based on different vegetal oils, by following a workflow consisting of in vitro and in vivo approaches, from the simplest to the more complex model.

This study confirms that functional O/W NEs based on Almond oil and Neem oil, capable of loading Vitamin E, are feasible in an appropriate range of relative concentration. The amount of each component in the NEs is chosen to obtain the highest content of oil, to enhance the biological effect, and the lowest amount of surfactant, to minimize the toxic effect of the selected formulations. The selected formulations are homogeneous and stable over time.

Both Almond-based and Neem-based NEs display the same in vitro release profile, possibly reflecting the similarity of the VitE-NEs, which appears to cancel the discrepancies in the morphology and structure of the unloaded NEs, as detected by SAXS and TEM.

Furthermore, NEs loaded with the same amount of Vitamin E display good and comparable antioxidant effect on in vitro keratinocyte monolayers and in vivo *C. elegans*, through a dose-dependent response.

Remarkably, when evaluated in in vivo studies on healthy volunteers, while both well tolerated, only Neem oil-based NEs displayed a prompt and efficient anti-inflammatory effect, seemingly synergic when loaded with VitE. The obtained results had surprisingly showed different behaviour of Neem oil- and Almond-based NEs: in detail, the cutaneous recovery after treatment with Almond-based NEs was superposable to the physiological one obtained with saline solution; on the contrary, Neem oil-based NEs were able to markedly reduce the erythema index already after 1 hour, accelerating the skin recovery. The synergistic effect of Neem-based NEs and VitE could be related to a higher skin penetration and retention propensity than the Almond formulations.

The obtained results seem to promote Neem oil over Almond oil as an appropriate candidate for further studies on the transport of VitE into skin to gain a deep understanding of an effective skin NEs/drug transport.

Abbreviations

ROS, reactive oxygen species; NEs, nanoemulsions; O/W, oil in water; VitE, Vitamin E; HaCaT, normal human keratinocytes; *C. elegans, Caenorhabditis elegans*; DLS, dynamic light scattering; SAXS, small-angle x-ray scattering; TEM, transmission electron microscopy; PDI, polydispersity index; DPH, 1.6-Diphenyl-1,3,5-hexatriene; MTT, 3-(4,5-dimethylthiazol-2-yl)-2,5-diphenyltetrazolium bromide; EI, Erythema index.

Acknowledgments

Disclosure

The authors report no conflicts of interest in this work.

References

1. Yoshikawa T, Naito Y. What is oxidative stress? *Japan Med Assoc J.* 2002;45(7):271–276.
2. Halliwell B. Phagocyte-derived reactive species: salvation or suicide? *Trends Biochem Sci.* 2006;31(9):509–515. doi:10.1016/j.tibs.2006.07.005
3. Halliwell B. The antioxidant paradox. *Lancet.* 2000;355(9210):1179–1180. doi:10.1016/S0140-6736(00)02075-4
4. Halliwell B. Biochemistry of oxidative stress. *Biochem Soc Trans.* 2007;35(5):1147–1150. doi:10.1042/BST0351147
5. Halliwell B, Gutteridge J. *Free Radicals in Biology and Medicine.* 4th ed. Oxford: Oxford University Press; 2007.
6. Halliwell B. Reactive species and antioxidants. Redox biology is a fundamental theme of aerobic life. *Plant Physiol.* 2006;141(2):312–322. doi:10.1104/pp.106.077073

7. Halliwell B, Gutteridge J. The definition and measurement of antioxidants in biological systems. *Free Radic Biol Med*. 1995;18(1):125–126. doi:10.1016/0891-5849(95)91457-3

8. Bast A, Goris R. Oxidative stress. *Pharm Weekbl*. 1989;11(6):199–206. doi:10.1007/BF01959411

9. Zaffarin ASM, Ng S-F, Ng MH, Hassan H, Alias E. Pharmacology and pharmacokinetics of vitamin E: nanoformulations to enhance bioavailability. *Int J Nanomedicine*. 2020;15:9961. doi:10.2147/IJN.S276355

10. Sies H. Strategies of antioxidant defense. *EJB Rev*. 1993;1994:101–107.

11. Feki M, Souissi M, Mebazaa A. Vitamin E deficiency: risk factor in human disease? *Annales de medecine interne*. 2001;152:398–406.

12. Nachbar F, Korting H. The role of vitamin E in normal and damaged skin. *J Mol Med*. 1995;73(1):7–17. doi:10.1007/BF00203614

13. Vaz S, Silva R, Amaral M, Martins E, Lobo JS, Silva A. Evaluation of the biocompatibility and skin hydration potential of vitamin E-loaded lipid nanosystems formulations: in vitro and human in vivo studies. *Colloids Surf B Biointerfaces*. 2019;179:242–249. doi:10.1016/j.colsurfb.2019.03.036

14. Jiang Q. Natural forms of vitamin E: metabolism, antioxidant, and anti-inflammatory activities and their role in disease prevention and therapy. *Free Radic Biol Med*. 2014;72:76–90. doi:10.1016/j.freeradbiomed.2014.03.035

15. Reiter E, Jiang Q, Christen S. Anti-inflammatory properties of α-and γ-tocopherol. *Mol Aspects Med*. 2007;28(5–6):668–691. doi:10.1016/j.mam.2007.01.003

16. Kuriyama K, Shimizu T, Horiguchi T, Watabe M, Abe Y. Vitamin E ointment at high dose levels suppresses contact dermatitis in rats by stabilizing keratinocytes. *J Inflamm Res*. 2002;51(10):483–489. doi:10.1007/PL00012416

17. Jurado-Campos A, Soria-Meneses PJ, Sánchez-Rubio F, et al. Vitamin E delivery systems increase resistance to oxidative stress in red deer sperm cells: hydrogel and nanoemulsion carriers. *Antioxidants*. 2021;10(11):1780. doi:10.3390/antiox10111780

18. Alhasso B, Ghori MU, Conway BR. Systematic review on the effectiveness of essential and carrier oils as skin penetration enhancers in pharmaceutical formulations. *Sci Pharm*. 2022;90(1):14. doi:10.3390/scipharm90010014

19. Ren T, Li R, Zhao L, Fawcett JP, Sun D, Gu J. Biological fate and interaction with cytochromes P450 of the nanocarrier material, D-α-tocopheryl polyethylene glycol 1000 succinate. *Acta Pharm Sin B*. 2022;12:3156–3166. doi:10.1016/j.apsb.2022.01.014

20. McClements DJ. Nanoemulsions versus microemulsions: terminology, differences, and similarities. *Soft Matter*. 2012;8(6):1719–1729. doi:10.1039/C2SM06903B

21. Naseema A, Kovooru L, Behera AK, Kumar KP, Srivastava P. A critical review of synthesis procedures, applications and future potential of nanoemulsions. *Adv Colloid Interface Sci*. 2020;287:102318. doi:10.1016/j.cis.2020.102318

22. Valantina RS, Neelamegam P. Antioxidant potential in vegetable oil. *Res J Chem Environ*. 2012;16(2):87–94.

23. Hosny K, Asfour H, Rizg W, et al. Formulation, optimization, and evaluation of oregano oil nanoemulsions for the treatment of infections due to oral microbiota. *Int J Nanomedicine*. 2021;16:5465. doi:10.2147/IJN.S325625

24. Brahmachari G. Neem—an omnipotent plant: a retrospection. *Chembiochem*. 2004;5(4):408–421. doi:10.1002/cbic.200300749

25. Ahmad Z. The uses and properties of almond oil. *Complement Ther Clin Pract*. 2010;16(1):10–12. doi:10.1016/j.ctcp.2009.06.015

26. Gossé B, Amissa AA, Anoh Adjé F, Bobélé Niamké F, Ollivier D, Ito Y. Analysis of components of neem (Azadirachta indica) oil by diverse chromatographic techniques. *J Liq Chromatogr Relat Technol*. 2005;28(14):2225–2233. doi:10.1081/JLC-200064164

27. Rinaldi F, Hanieh PN, Longhi C, et al. Neem oil nanoemulsions: characterisation and antioxidant activity. *J Enzyme Inhib Med Chem*. 2017;32(1):1265–1273. doi:10.1080/14756366.2017.1378190

28. Bhowmik D, Chiranjib YJ, Tripathi K, Kumar KS. Herbal remedies of Azadirachta indica and its medicinal application. *J Chem Pharm Res*. 2010;2(1):62–72.

29. Bhargava K, Gupta M, Gupta G, Mitra C. Anti-inflammatory activity of saponins and ot-her natural products. *Indian J Med Res*. 1970;58(6):724–730.

30. Pillai N, Santhakumari G. Anti-arthritic and anti-inflammatory actions of nimbidin. *Planta Med*. 1981;43(09):59–63. doi:10.1055/s-2007-971474

31. Biswas K, Chattopadhyay I, Banerjee RK, Bandyopadhyay U. Biological activities and medicinal properties of neem (Azadirachta indica). *Curr Sci*. 2002;82:1336–1345.

32. Sarkar S, Singh RP, Bhattacharya G. Exploring the role of Azadirachta indica (neem) and its active compounds in the regulation of biological pathways: an update on molecular approach. *Biotech*. 2021;11(4):1–12. doi:10.1007/s13205-021-02745-4

33. Blum FC, Singh J, Merrell DS. In vitro activity of neem (Azadirachta indica) oil extract against Helicobacter pylori. *J Ethnopharmacol*. 2019;232:236–243. doi:10.1016/j.jep.2018.12.025

34. Maestri D, Martínez M, Bodoira R, et al. Variability in almond oil chemical traits from traditional cultivars and native genetic resources from Argentina. *Food Chem*. 2015;170:55–61. doi:10.1016/j.foodchem.2014.08.073

35. Mohammed SH, Hussein RH. Anti-hypertensive and anti-oxidant activities of walnut almond oil, and corn and candesartan on L-NAME induced hypertensive rats. *J Zankoy Sulaimani*. 2020;22:43–54. doi:10.17656/jzs.10806

36. Jaganathan SK, Mani MP. Morphological properties of almond oil constituted nanofibrous scaffold for bone tissue engineering. *Polym Polym Compos*. 2020;28(4):233–241. doi:10.1177/0967391119870413

37. Fasano E, Serini S, Mondella N, et al. Antioxidant and anti-inflammatory effects of selected natural compounds contained in a dietary supplement on two human immortalized keratinocyte lines. *Biomed Res Int*. 2014;2014. doi:10.1155/2014/327452

38. Telò I, Favero ED, Cantù L, et al. Gel-like TPGS-based microemulsions for imiquimod dermal delivery: role of mesostructure on the uptake and distribution into the skin. *Mol Pharm*. 2017;14(10):3281–3289. doi:10.1021/acs.molpharmaceut.7b00348

39. Back PI, Balestrin LA, Fachel FNS, et al. Hydrogels containing soybean isoflavone aglycones-rich fraction-loaded nanoemulsions for wound healing treatment–in vitro and in vivo studies. *Colloids Surf B Biointerfaces*. 2020;196:111301. doi:10.1016/j.colsurfb.2020.111301

40. Rupa EJ, Li JF, Arif MH, et al. Cordyceps militaris fungus extracts-mediated nanoemulsion for improvement antioxidant, antimicrobial, and anti-inflammatory activities. *Molecules*. 2020;25(23):5733. doi:10.3390/molecules25235733

41. Xiao L, Mochizuki M, Nakahara T, Miwa N. Hydrogen-generating silica material prevents UVA-ray-induced cellular oxidative stress, cell death, collagen loss and melanogenesis in human cells and 3D skin equivalents. *Antioxidants*. 2021;10(1):76. doi:10.3390/antiox10010076

42. Zagórska-Dziok M, Ziemlewska A, Bujak T, Nizioł-łukaszewska Z, Hordyjewicz-Baran Z. Cosmetic and dermatological properties of selected ayurvedic plant extracts. *Molecules*. 2021;26(3):614. doi:10.3390/molecules26030614

43. Schifano E, Zinno P, Guantario B, et al. The foodborne strain Lactobacillus fermentum MBC2 triggers pept-1-dependent pro-longevity effects in Caenorhabditis elegans. *Microorganisms*. 2019;7(2):45. doi:10.3390/microorganisms7020045

44. Ghotbi RS, Khatibzadeh M, Kordbacheh S. *Preparation of Neem Seed Oil Nanoemulsion*. Proceedings of the 5th International Conference on Nanotechnology: Fundamentals and Applications; 2014:11–13.

45. Silva AL, Marcelino HR, Veríssimo LM, Araujo IB, Agnez-Lima LF, Do Egito EST. do Egito ES. Stearylamine-containing cationic nanoemulsion as a promising carrier for gene delivery. *J Nanosci Nanotechnol*. 2016;16(2):1339–1345. doi:10.1166/jnn.2016.11671

46. Di Cola E, Brocca P, Rondelli V, et al. Novel O/W nanoemulsions for nasal administration: structural hints in the selection of performing vehicles with enhanced mucopenetration. *Colloids Surf B Biointerfaces*. 2019;183:110439. doi:10.1016/j.colsurfb.2019.110439

47. Doucet M, Cho JH, Alina G, et al. SasView Version 4.1, Zenodo; 2017.

48. Di Marzio L, Marianecci C, Cinque B, et al. pH-sensitive non-phospholipid vesicle and macrophage-like cells: binding, uptake and endocytotic pathway. *Biochimica et Biophysica Acta*. 2008;1778(12):2749–2756. doi:10.1016/j.bbamem.2008.07.029

49. Bains GK, Kim SH, Sorin EJ, Narayanaswami V. The extent of pyrene excimer fluorescence emission is a reflector of distance and flexibility: analysis of the segment linking the LDL receptor-binding and tetramerization domains of apolipoprotein E3. *Biochemistry*. 2012;51(31):6207–6219. doi:10.1021/bi3005285

50. Brenner S. The genetics of Caenorhabditis elegans. *Genetics*. 1974;77(1):71–94. doi:10.1093/genetics/77.1.71

51. Schifano E, Marazzato M, Ammendolia MG, et al. Virulence behavior of uropathogenic Escherichia coli strains in the host model Caenorhabditis elegans. *MicrobiologyOpen*. 2019;8(6):e00756. doi:10.1002/mbo3.756

52. Paolino D, Lucania G, Mardente D, Alhaique F, Fresta M. Ethosomes for skin delivery of ammonium glycyrrhizinate: in vitro percutaneous permeation through human skin and in vivo anti-inflammatory activity on human volunteers. *J Control Release*. 2005;106(1–2):99–110. doi:10.1016/j.jconrel.2005.04.007

53. Syed HK, Peh KK. Identification of phases of various oil, surfactant/co-surfactants and water system by ternary phase diagram. *Acta Pol Pharm*. 2014;71(2):301–309.

54. Kumar N, Mandal A. Thermodynamic and physicochemical properties evaluation for formation and characterization of oil-in-water nanoemulsion. *J Mol Liq*. 2018;266:147–159. doi:10.1016/j.molliq.2018.06.069

55. Saberi AH, Fang Y, McClements DJ. Fabrication of vitamin E-enriched nanoemulsions: factors affecting particle size using spontaneous emulsification. *J Colloid Interface Sci*. 2013;391:95–102. doi:10.1016/j.jcis.2012.08.069

56. Azeem A, Rizwan M, Ahmad FJ, et al. Nanoemulsion components screening and selection: a technical note. *Aaps Pharmscitech*. 2009;10(1):69–76. doi:10.1208/s12249-008-9178-x

57. Pavoni L, Perinelli DR, Ciacciarelli A, et al. Properties and stability of nanoemulsions: how relevant is the type of surfactant? *J Drug Deliv Sci Technol*. 2020;58:101772. doi:10.1016/j.jddst.2020.101772

58. Klang V, Valenta C. Lecithin-based nanoemulsions. *J Drug Deliv Sci Technol*. 2011;21(1):55–76. doi:10.1016/S1773-2247(11)50006-1

59. Coors EA, Seybold H, Merk HF, Mahler V. Polysorbate 80 in medical products and nonimmunologic anaphylactoid reactions. *Ann Allergy Asthma Immunol*. 2005;95(6):593–599. doi:10.1016/S1081-1206(10)61024-1

60. Mishra L, Gupta S. Fluconazole and curcumin loaded nanoemulsion against multiple drug resistance dermatophytes. *Biomed Pharmacol J*. 2021;14 (4):2085–2094. doi:10.13005/bpj/2305

61. Azizi M, Esmaeili F, Partoazar A, Ejtemaei Mehr S, Amani A. Efficacy of nano-and microemulsion-based topical gels in delivery of ibuprofen: an in vivo study. *J Microencapsul*. 2017;34(2):195–202. doi:10.1080/02652048.2017.1316324

62. Wakisaka S, Nakanishi M, Gohtani S. Phase behavior and formation of o/w nano-emulsion in vegetable oil/mixture of polyglycerol polyricinoleate and polyglycerin fatty acid ester/water systems. *J Oleo Sci*. 2014;63:ess13139.

63. Abdollahi E, Momtazi AA, Johnston TP, Sahebkar A. Therapeutic effects of curcumin in inflammatory and immune-mediated diseases: a nature-made jack-of-all-trades? *J Cell Physiol*. 2018;233(2):830–848. doi:10.1002/jcp.25778

64. Abla M, Banga A. Formulation of tocopherol nanocarriers and in vitro delivery into human skin. *Int J Cosmet Sci*. 2014;36(3):239–246. doi:10.1111/ics.12119

65. Harun MS, Wong TW, Fong CW. Advancing skin delivery of α-tocopherol and γ-tocotrienol for dermatitis treatment via nanotechnology and microwave technology. *Int J Pharm*. 2021;593:120099. doi:10.1016/j.ijpharm.2020.120099

66. Atrux-Tallau N, Delmas T, Han SH, Kim JW, Bibette J. Skin cell targeting with self-assembled ligand addressed nanoemulsion droplets. *Int J Cosmet Sci*. 2013;35(3):310–318. doi:10.1111/ics.12044

67. Mericli F, Becer E, Kabadayı H, et al. Fatty acid composition and anticancer activity in colon carcinoma cell lines of Prunus dulcis seed oil. *Pharm Biol*. 2017;55(1):1239–1248. doi:10.1080/13880209.2017.1296003

68. Aan GJ, Zainudin MSA, Karim NA, Ngah WZW. Effect of the tocotrienol-rich fraction on the lifespan and oxidative biomarkers in Caenorhabditis elegans under oxidative stress. *Clinics*. 2013;68(5):599–604. doi:10.6061/clinics/2013(05)04

69. Ristow M, Schmeisser S. Extending life span by increasing oxidative stress. *Free Radic Biol Med*. 2011;51(2):327–336. doi:10.1016/j.freeradbiomed.2011.05.010

70. Denzel MS, Lapierre LR, Mack HI. Emerging topics in C. elegans aging research: transcriptional regulation, stress response and epigenetics. *Mech Ageing Dev*. 2019;177:4–21. doi:10.1016/j.mad.2018.08.001

71. Roselli M, Schifano E, Guantario B, Zinno P, Uccelletti D, Devirgiliis C. Caenorhabditis elegans and probiotics interactions from a prolongevity perspective. *Int J Mol Sci*. 2019;20(20):5020. doi:10.3390/ijms20205020

72. Luo Y. Long-lived worms and aging. *Redox Rep*. 2004;9(2):65–69. doi:10.1179/135100004225004733

73. Schifano E, Ficociello G, Vespa S, et al. Pmr-1 gene affects susceptibility of Caenorhabditis elegans to staphylococcus aureus infection through glycosylation and stress response pathways' alterations. *Virulence*. 2019;10(1):1013–1025. doi:10.1080/21505594.2019.1697118

74. Zhang L, Gu B, Wang Y. Clove essential oil confers antioxidant activity and lifespan extension in C. elegans via the DAF-16/FOXO transcription factor. *Comp Biochem Physiol*. 2021;242:108938.

75. Schlotterer A, Masri B, Humpert M, Krämer BK, Hammes H-P, Morcos M. Sulforaphane and vitamin E protect from glucotoxic neurodegeneration and lifespan reduction in C. elegans. *Exp Clin Endocrinol Diabetes*. 2021;129(12):887–894. doi:10.1055/a-1158-9248

76. Naik MR, Bhattacharya A, Behera R, Agrawal D, Dehury S, Kumar S. Study of anti-inflammatory effect of neem seed oil (Azadirachta indica) on infected albino rats. *J Health Res*. 2014;1(3):66. doi:10.4103/2394-2010.153880

77. Dutta G, Deori C, Das S. Anti-inflammatory activity of ethanolic extract of Azadirachta indica leaves on experimental animal models. *J Evol Med Dent Sci*. 2016;5(85):6335–6339. doi:10.14260/Jemds/2016/1431

78. Emran T, Nasir Uddin M, Rahman A, Uddin Z, Islam M. Phytochemical, antimicrobial, cytotoxic, analgesic and anti-inflammatory properties of Azadirachta indica: a therapeutic study. *J Bioanal Biomed S.* 2015;12:2.

79. Amra K, Momin M, Desai N, Khan F. Therapeutic benefits of natural oils along with permeation enhancing activity. *Int J Dermatol.* 2022;61 (4):484–507. doi:10.1111/ijd.15733